Transactions of the **14th International Conference on Structural Mechanics in Reactor Technology** (SMiRT 14), Lyon, France, August 17-22, 1997

Size effects on tensile impact mechanical properties and fracture process of plain concrete

Albertini C., Cadoni E., Economou S., Labibes K.
European Commission - Joint Research Centre - ISIS, Italy

ABSTRACT

In order to study the mechanical behaviour of plain concrete at high strain rates a new experimental methodology has been developed. This new technique concerns the tensile behaviour of concrete and recommends a development of the well known Hopkinson's bar technique for testing large specimen. This paper describes the experiment and its capability of measuring the mechanical properties and the fracture process of plain concrete with large size aggregate under high loading rate and compares with those obtained from microconcrete having aggregate size of 5-10 mm. The descriptionof the experimental results by strain rate dependent model for concrete under dynamic loading is also presented.

INTRODUCTION

For the safe design of concrete containment shell in nuclear reactors a realistic estimation of material properties is needed, especially, when the structures are subject to severe accidental loads (i.e. earthquake, impact or explosion). Code previsions used by now are tending to be very conservative in order to fill the gap of missing knowledge of material behaviour under the above mentioned loading conditions. Application of fracture mechanics concepts for failure prediction under dynamic loads, as well as, definition of failure criteria in order to reproduce the actual material behaviour needs realistic estimation of characteristic material parameters. The need emerges for accurate measurement of the material behaviour, representative of loading conditions likely to be occurred in its lifetime. So, in order to measure the mechanical behaviour of plain concrete at high strain rates a new test methodology is proposed. A series of experiments on plain concrete cubes of 200 and 60 mm side with maximum aggregate size of 25 mm have been carried out at the Joint Research Centre - Ispra. Specimens have been tested by means of Hopkinson Bar Bundle (HBB). This bar consists of a bundle of 25 elementary Hopkinson bars working in parallel over the cross-section of the large specimen.

EXPERIMENTAL TECHNIQUE

The Hopkinson bar technique is a widely used technique to determine mechanical properties of structural materials under high loading rates. While, standard Hopkinson bars [1,2] with a diameter in the range of 10-20 mm are sufficient for dynamic testing of fine-grained materials (i.e. steel), larger bars are needed to test concrete specimens with real-size aggregates. Moreover, special equipment is needed for the observation of stress and strain distribution over the cross-section of large concrete specimens. These distributions are actually not uniform over the section, due to material cracking while it is loaded.

To study dynamic properties of plain concrete, a special Hopkinson bar bundle (HBB) has been developed and installed in the Large Dynamic Testing Facility (LDTF) [3] of the Joint Research Centre at Ispra (Fig. 1).

The HBB is a special equipment enabling for the correct characterisation of the stress-strain diagram, as well as for the evaluation of energy absorption during fracture of concrete specimens. The device consists of two bundles of 25 aluminum bars among which the specimen is glued with an epoxy resin, as shown in Fig. 1. Bar bundles are made of aluminum and are 2 m long with a square section of 200 mm side. They are further subdivided by electroerosion into 25 symmetrical pairs of parallel bars for the first half (1 m) while the rest remains as whole. Concrete specimens are tested with the same section as the aluminum bar. Putting strain gauges on each individual bar of the bundle, measures of the incident, reflected and transmitted pulses are obtained, concerning each prismatic portion of specimen which is included between the symmetric pair of bars of the bundles. The entire parts of the bars are also instrumented to measure incident, reflected and transmitted pulses considered to the specimen as a whole homogeneous material.

The bar developed in our laboratory differs the traditional Hopkinson device in the fact that, the incident mechanical pulse is generated by the sudden release of the energy stored in 32 cables of high strength steel and not by impacting projectile. Further, as Morse [4] has shown, the longitudinal wave propagation through a square section bar is equal to that in the cylindrical section.

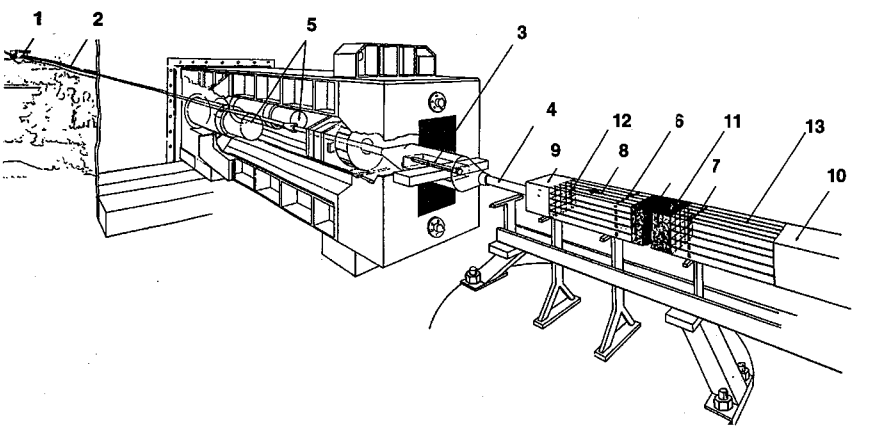

Fig. 1 - Experimental set-up : 1. hydraulic actuator; 2. high strength steel cables for energy storage (100m); 3. explosive bolt; 4. loading bar; 5. hydraulic dampers; 6. strain gauges to measure incident and reflected pulses; 7. strain gauges to measure transmitted pulses; 8. load direction; 9. instrumented input whole bar; 10. instrumented output whole bar; 11. specimen; 12 elementary input bar bundle; 13. elementary output bar bundle.

A test with the LDTF-HBB is scheduled to be performed as follows:

1) an hydraulic actuator, of maximum loading capacity of 5 MN, is pulling 32 cables of high strength steel, each one 100 m long; the prestress force is resisted by one grounded explosive bolt in the blocking device (see Fig. 1);

2) rupturing the explosive bolt means the onset of a tensile pulse of 40 ms duration with linear loading rate during the rise time, which propagates along the bar and causes specimen fracture.

Strain gauge stations on input bars measure incident ε_I , and reflected ε_R , pulses. Strain-gauge stations on the output bars measure transmitted pulses ε_T.

The lengths of input and output bar, glued to the specimen, guarantee that wave reflections over bar ends not reach the specimen before its failure. Also, the assumption of uniaxial elastic wave propagation theory is fulfilled because, the pulse wavelength (100m) is much longer than the transversal length of the bar (~0.3 m). When the specimen is reasonably short, the travel time of the elasto-plastic wave through the specimen is small in comparison to the test duration, so it can be considered as being in equilibrium and under uniform stress-state due to the many wave reflections between its ends.

These assumptions are employed to calculate the average stress and strain time histories for concrete subjected to different strain-rate time histories. The following equations [1,2] are used:

$$\sigma(t) = E\frac{A}{A_s}\varepsilon_T(t) \quad (1); \qquad \varepsilon(t) = -\frac{2\,c_0\int_0^t \varepsilon_R\,dt}{L_s} \quad (2); \qquad \varepsilon(t) = -\frac{2C_0}{L_s}\varepsilon_R(t) \quad (3)$$

where: E = aluminum bar Young modulus; A = bar cross section; A_S = specimen cross section; C_0 = bar wave speed; L_S = specimen length; t = time.

The two different strain-gauge stations (one on the entire bar and the other on each prismatic bar of the subdivided part), are used to determine σ and ε together with records of an electro-optical device which measures the displacement of the specimen ends. In Figs. 2 and 3, records of incident and transmitted pulses are presented, respectively.
Records from each elementary bar of the bundle are used to interpret concrete behaviour both at local and global level [5].

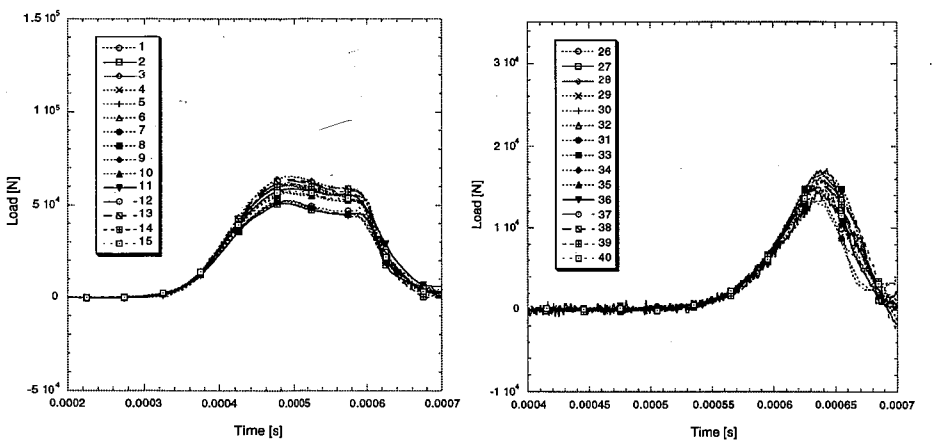

Figs. 2-3 - Records from the incident and transmitted bar bundle

SIZE EFFECT ON TENSILE MECHANICAL PROPERTIES OF PLAIN CONCRETE

Size effects principally reflect the material inhomogeneity (i.e. for a perfectly homogeneous material there are not any). It is therefore logical to correlate measurements of concrete mechanical parameter with its specimen dimensions. Following Weibull's model [6], the larger the volume of the specimen the most likely an element exhibit the lowest strength. In other words, increasing the size of specimen increases also the probability to observe a smaller strength. Experiments were performed on small specimens (60x60 mm) with the same cement

content as the large ones (200*200 mm) on a similar bar. The mean stress vs. strain curves for these two cases are shown in Fig. 4. It is possible to observe that maximum stress and strain are different for the two specimen sizes for the same strain-rate.

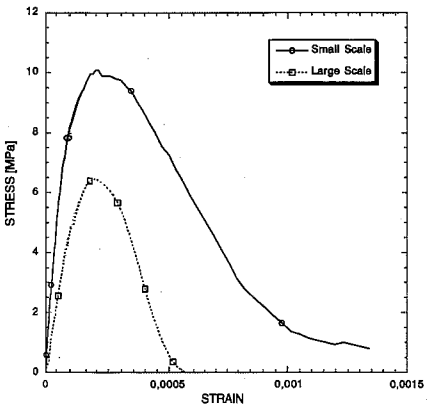

Fig. 4 - Stress vs. strain curves of large and small specimen (strain rate = 10 s^{-1})

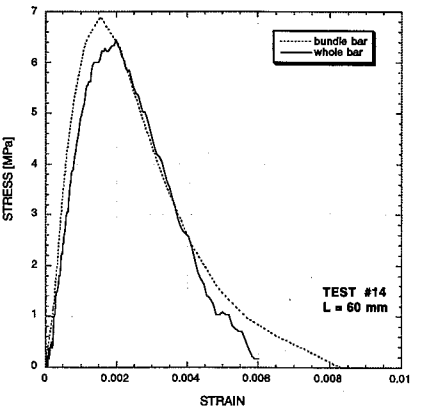

Fig. 5 - Comparison between the stress vs. strain curve calculated in two different modes

DEFINITION OF THE TRUE STRESS-STRAIN CURVES

The stress-strain curve has been determined in two different ways. In the first: the stress was calculated using eq. (1) with values of ε_T coming from the strain gauge of the whole output bar, while strain was measured by means of the electro-optical device. In the second, the stress measured from the transmitter bundle bars, as the average of these, and the strain as the average of the strains calculated from the reflected waves measured in the incident bundle bars. This second way is presented in the following.

The instantaneous values of the stress and strain of the concrete facing the Nth elementary Hopkinson bar of the bundle are obtained by the following equations:

$$\sigma_N(t) = \frac{A_N \cdot E \cdot \varepsilon_{T_N}(t)}{A_0} \quad (4); \qquad \varepsilon_N(t) = \frac{2C}{L_0}\int_0^t \varepsilon_{R_N}(t)\,dt \quad (5)$$

where: A_N = cross-section of the Nth elementary aluminum bar; A_O = cross-section of the concrete facing the elementary Hopkinson bar; E = Young modulus of aluminum; t= time; C= elastic wave speed in aluminum; L_O = length of the concrete specimen.

During the test time the fractured parts of the specimen cross-section reduce to zero the records ε_{T_N} (or ε_{R_N} =- ε_{I_N}) of the facing transmitter bars of the bundle and therefore the corresponding values of eq.(4); then, we can assume as first approximation that the true stress and true strain of the specimen are given by the average of the stresses and strains of the X bars of the bundle where $\varepsilon_{T_N} \neq 0$, as follows:

$$\sigma_{TRUE}(t) = \frac{\dfrac{\sum_1^X A_N \cdot E \cdot \varepsilon_{T_N}(t)}{A_0}}{X} \quad (6)\ ; \quad \varepsilon_{TRUE}(t) = \frac{\sum_1^X \dfrac{2C}{L_0}\int_0^t \varepsilon_{R_N}(t)\,dt}{X} \quad (7)$$

Stress-strain curves determined following the above mentioned two modes (whole and bundle bar records) as described previously are compared in Fig. 5. It can be seen that they differ a little. Strength and the softening branch of the stress-strain curve calculated with the second way are higher than those calculated with the first one. The difference arises from the more detailed analysis allowed by the bar bundle method and it is not big because fracture starts simultaneously in many points of specimen cross section.
The strain rate of the tests was 10 s^{-1}.

Consider that the concrete part facing the Nth bar of the bundle begins to fracture when the corresponding transmitted pulse ε_{T_N} reaches its maximum and starts decreasing to zero; then, Figs 6-7 give time and corresponding crack initiation over specimen cross-section using the above condition. It can be seen that:

- in ten microseconds the crack initiation spreads over the whole specimen cross-section revealing the multiactivation mode of the fracture process;
- the initiation of the first crack at 121 μs corresponds to the beginning of the loss of linearity of the ascending branch of the total loading;
- the spread time of the crack initiation over the whole cross-section (from 121 to 131 μs) corresponds to the begin of the total loading softening branch.

Taking into account these observations, a method for the determination of the true stress-strain diagram, based on the bar bundle records, is proposed. This refined method, introduces for the specimen a value of the residual resisting cross-section A_{TRUE} which is less than the initial value A_0 , and is calculated as a function of the damage induced in the specimen due to crack propagation.

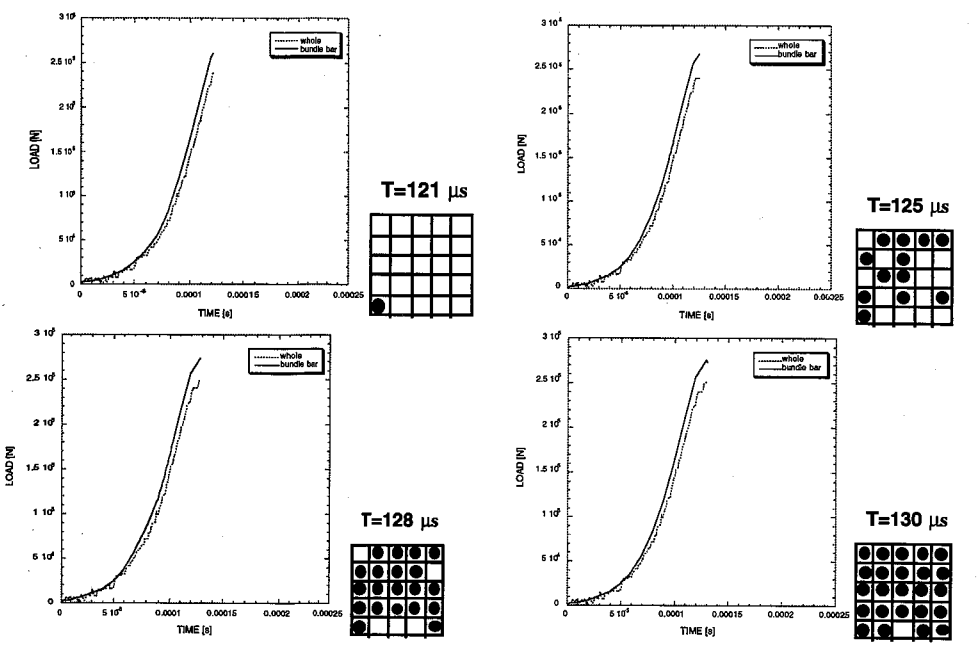

Figs. 6-7 - Total load vs. time curves of the bundle bar and whole bar compared with crack initiation when ε_{T_N} = max

For the estimation of A_{TRUE} a signal of a generic transmitter bundle bar is considered where it is possible to recognise two characteristic points. Points t_1 and t_2 represent time corresponding to maximum and the final zero value of ε_{T_N} respectively. It is assumed that during Δt ($\Delta t = t_1 - t_2$) the residual resisting cross-section of the elementary bar decreases linearly with time t from the initial value A_0 to zero. This decrease is assumed as a linear function of time, $f_N(t)$:

$$f_N(t) = 1 - \frac{t - t_1}{t_2 - t_1} \qquad \text{with} \qquad t_1 \le t \le t_2$$

This assumption is confirmed by the observation of records of transmitted pulse ε_{T_N} in Fig.3. Therefore the total residual resisting cross-section of the specimen and the total load P_{true} from the bundle bars are given as:

$$A_{true} = \sum_{N=1}^{25} A_0 \cdot f_N(t) \qquad (8) \qquad ; \qquad P_{true} = \sum_{N=1}^{25} A_N \cdot E \cdot \varepsilon_{T_N} \qquad (9)$$

where: A_O = cross-section of the specimen facing the Nth bar; A_N = cross-section area of an elementary aluminum bundle bar; E = aluminum elastic modulus; ε_{T_N} = transmitted pulse in an elementary bar bundle

Then, the true stress σ_{true} of concrete is calculated as follows:

$$\sigma_{true} = \frac{P_{true}}{A_{true}} = \frac{\sum_{N=1}^{25} A_N \cdot E \cdot \varepsilon_{T_N}}{\sum_{N=1}^{25} A_0 \cdot f_N(t)} \qquad (10)$$

In this method estimation of true stress-strain diagram, strain is calculated by eq. (7). In Fig. 8 the true stress-strain curves are shown. The solid curve has been obtained with the refined method by applying eqs. (10) and (7) to the records of the bar bundles. The curve with the dotted line has been obtained by the applying eqs. (6) and (7). The comparison shows that, the refined method gives a more precise description of the softening branch of the stress-strain diagram for concrete, as well as for the energy absorption capability of the material during fracture.

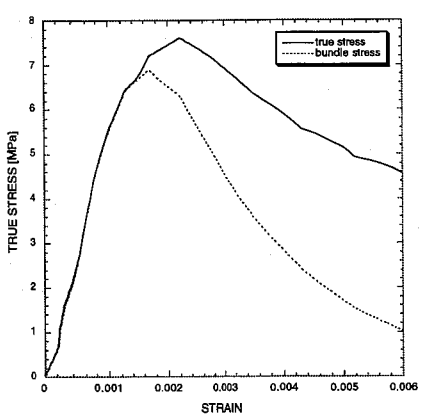

Fig. 8 - True stress vs. strain curves by two methods of bar bundle analysis. Specimen #14

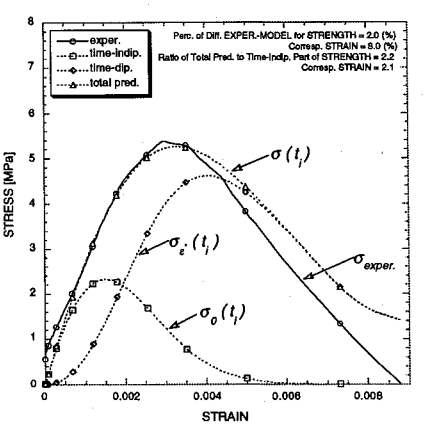

Fig. 9 - Experimental vs. predicted stress-strain curves

CONSTITUTIVE MODEL FOR TENSION

A rational mechanical model primarily based on inertia effects, proposed by Bachmann[7], has been further developed and implemented to reproduce the observed experimental behaviour of concrete under different strain-rates. The model takes into account: a) nonlinear behaviour with respect to an internal damage parameter, where the location and the amount of damage are distributed stochastically; b) loading and unloading regarding internal friction; and c) damage due to microcracking inertia effects. The model is very briefly described in the following:

Stress is assumed to be determined at each time point as the sum of a time-independent part $\sigma_o(\varepsilon_i)$, and of a time-dependent one $\sigma_{\dot{\varepsilon}}(t_i)$:

$$\sigma(t_i) = \sigma_o(\varepsilon_i) + \sigma_{\dot{\varepsilon}}(t_i) \tag{11}$$

The first part, $\sigma_o(\varepsilon_i)$, depends only on the momentary strain ε_i, at time t_i:

$$\sigma_o(\varepsilon_i) = E \cdot \varepsilon_i \cdot e^{-\left(\frac{\varepsilon_i - \varepsilon_o}{\delta}\right)^{\gamma}} \tag{12}$$

E: Young modulus for concrete under tension; Exponential term expresses non-linear behaviour (i.e. internal damage parameter). For concrete with compressive strength f_{cu}=50.4 MPa, we have ε_o= -1.10^{-4}, δ = 2.8 10^{-4}, and γ=2.1). The second part, $\sigma_{\dot{\varepsilon}}(t_i)$, depends on strain and strain-rate time history up to the specific time point t_i:

$$\sigma_{\dot{\varepsilon}}(t_i) = k_m \cdot \sum_{j=1,i} \left[\Delta_{\alpha_j} \cdot \max\left(\eta_j + \eta_{gj}, \frac{k_1 \cdot S_{\beta j}}{k_m} \right) \right]$$
$$\Delta_{\alpha j} = e^{-\left(\frac{\varepsilon_j - \varepsilon_o}{\delta}\right)^{\gamma}} - e^{-\left(\frac{\varepsilon_{j-1} - \varepsilon_o}{\delta}\right)^{\gamma}} \tag{13}$$

The time-dependent term takes into account internal friction and inertia effects over the material volume due to the existing microcracking. The mechanical model takes care of these effects in the following way: Assumes a series of horizontal 1-D springs arranged in parallel, over the structural system which undergoes the externally applied load; In the interior of each spring two masses are connected between them and also to the borders; Each spring can be found in two potential states: a) Before crack initiation: masses are not activated (like not existing), and the only spring between the structural borders, is being in an elastic state; b) After crack initiation: Spring force S_f exceeds a predefined level S_b, so, crack initiates for the specific system and the spring connecting the two masses breaks, the two masses (m) are activated and the two springs which connect them to the borders also, showing a new stiffness k_m. The borders which represent the rest of the structural system have a much bigger mass than the two internal masses (m), and inertia effects are introduced for the rest of the time-dependent response. This means that due to inertia, when the border moves towards one spatial direction, $n_g(\tau)$, the mass lags behind this movement by n(t), reducing the overall actual deformation of the system. This appears as an overstress factor of the material and explains the observed dynamic strength increase of concrete.

Tensile tests performed at LDTF provide strain and strain-rate time-histories which along with mechanical and geometric characteristics of the specimen form the input for the constitutive equations. In Fig. 9, experimental σ–ε curve is compared to the predicted one, by means of strength, corresponding strain, ratios of dynamic to static strength and strain. The

agreement between model and experiment is very good. The constitutive model is being presented much more analytically in [8], where it is also concluded the very interesting agreement with test results. Further, the model was extended to describe the compressive behaviour of concrete under high strain-rates.

CONCLUSIONS

The HBB technique allows to define accurately the stress-strain diagram of concrete especially in the softening branch. It has been measured step by step: the true resisting cross-section and the load acting on that cross-section; the displacement given by the deformation of the true resisting cross-section; the crack propagation path and speed.
These parameters were used to determine the true stress-strain diagram and of the fracture process up to the complete separation of the specimen in two halves.
It has also been shown that, using this technique makes possible to follow in detail the impact fracture propagation process and to correlate local morphology of the specimen with the local measurement of mechanical characteristics. It has also been observed that increasing the size of the specimen, the strength decreases, which means that also in dynamic concrete behaviour the size effects exists.
Present results are part of a larger research programme which also includes, the study of relative humidity effects on concrete properties as well as dynamic behaviour of concrete under compressive loading.

REFERENCES

1. Davies, R.M. 1948, A Critical Study of the Hopkinson Pressure Bar, *Phil. Trans.Roy. Soc.*, London, Ser. A, 240-375.
2. Lindholm, U.S. 1971, *High Strain Rate Test*, Techinque of Metals Research (Wiley),Vol. 5, Part. 1.
3. Albertini, C., Montagnani, M. 1979, Testing Technique in Dynamic Biaxial Loading, (Institute of Physics, London) Conf.Ser.No. 47, 25-34.
4. Morse, R. W. 1948, J. Acoust. Soc Amer., 20, 833.
5. Albertini, C., Cadoni, E., Labibes, K. 1996, Dynamic mechanical behaviour of large concrete specimen by means of a bundle Hopkinson bars, Proc. *2nd ISIE*: 214-219, Beijing.
6. Weibull , W. 1951, A statistical distribution function of wide applicability, *Journal Appl. Mech.*,18, pp. 293-297.
7. Bachmann, H. 1993, Die Massentragheit in einem Pseudo-Stoffgesetz fur Beton dei schneller Zugbeanpruchung, Massivbau Baustofftechnologie Karlsr, H19.
8. Economou, S., Cadoni, E., Labibes, K., Albertini, C. 1996, Strain-Rate Effects on Plain Concrete in Tension, Proc. XXV AIAS, 4-7 Sept. '96, Gallipoli (Italy), vol.2, pp. 1229-1237.